UJEAS

UNIZIK JOURNAL OF ENGINEERING AND APPLIED SCIENCES

UNIZIK Journal of Engineering and Applied Sciences 5(1), June (2025), 2345 - 2363
Journal homepage: https://journals.unizik.edu.ng/index.php/ujeas
PRINT ISSN: 2992-4383 || ONLINE ISSN: 2992-4391

# Environmental Impact and Optimization of Bio-Hydraulic Fluid from Biobased oil and Friction modifiers (Eggshell and Snail shell)

Ifediorah E. I* and Ezeugo J. O
Department of Chemical Engineering, Chukwuemeka Odumegwu Ojukwu University, Nigeria.
*Corresponding Author's E-mail: Ezekielifediorah@gmail.com

**Abstract**
This work investigated the use of eggshells and snail shells as bio-friction modifiers compared to graphite in formulating bio-hydraulic fluids from palm oil, to improve environmental sustainability. Glycerol was produced through the transesterification of palm oil and characterised using Gas Chromatography-Mass Spectrometry (GC-MS). Graphite, eggshells, and snail shells were characterised using X-ray Diffraction (XRD). Three samples of separately formulated bio-hydraulic fluids from graphite, eggshells, and snail shells were characterised to ascertain the values of the pour point, flash point, viscosity, and biochemical oxygen demand. The functional groups of the bio-hydraulic fluids were identified using Fourier Transform Infrared Spectroscopy (FTIR) and optimised using Response Surface Methodology (RSM). The GCMS analysis of glycerol identified key chemical constituents (including dihydro-2-methyl-3-furanone, neopentyl glycol, and linoleic acid) essential for lubricity. The XRD analysis revealed eggshells and snail shells possessed mineralogical properties (calcite and aragonite respectively), confirming their suitability as friction modifiers. FTIR spectra of the bio-hydraulic fluids identified key functional groups (alkanes, heteroatoms) demonstrating suitability for hydraulic applications. The optimised bio-hydraulic fluid viscosity and its process conditions were given as: dynamic viscosity 34.78, 31.95, 33.48 cP; glycerol/methanol ratio 20:20:20; eggshell dosage 0.6/0.6/0.6 g; temperature 60/60/60°C; and time 30/30/30 min, for graphite, eggshell, and snail shell respectively. Achieving predictive accuracy ($R^2 \approx 0.99$), with a margin of error of less than 5%, shows that the quadratic model generated is accurate in prediction. The physicochemical properties of the formulated fluid were: pour point -44.8, -41.7, -40.5°C; flash point 257, 249, 246°C; biochemical oxygen demand (BOD) 8.23, 8.04, 8.11 ppm, for graphite, eggshell, and snail shell respectively. The formulated bio-hydraulic fluids perform better in pour point, flash point, and BOD compared to mineral-based fluids, while matching bio-based fluid standards for viscosity. These properties, validated by ASTM standards, confirm the potential of palm oil, eggshell, and snail shell as sustainable eco-materials for hydraulic fluid applications.

**Keywords:** Bio-hydraulic fluid, Friction modifiers, FT-IR, Optimization, Palm oil

## 1.0 Introduction

Hydraulic fluids are lubricants that support the efficiency of machine parts. The hydraulic fluid used as an energy transmission agent and in the management of hydraulic components is one of the factors that determines the lifetime, durability, and dependability of any hydraulic system. Bio-hydraulic lubricants function as anti-wear, anti-rust, and anti-oxidants in the hydraulic system. Currently, synthetic ester (like polyol ester) and vegetable oils (such as rapeseed, sunflower, corn, soybean, canola, coconut, etc.) are used to make these bio-based hydraulic fluids together with other additives. Their lubricating qualities are quite comparable to those of mineral oils; they are biodegradable and pose low environmental risk, Deuster, *et al*., (2021) and Behzad, et al., (2024).

Eggshell waste is an abundant natural waste, and it is a significant waste of the food industry, with the U.S. generating approximately 150,000 tons of eggshell waste annually and Taiwan's egg industry used about 50 million crates of egg and leaving over 120 tons of eggshell as waste Mignardi, et al., (2020). Fichtelite (42.27%), hanksite (35,07%), and calcite (11.06%) make egg shells suitable for viscosity modifiers. In 2022, the snail foods and delicacies market was

projected to be valued at USD 593.4 million worldwide. The market is anticipated to expand at a compound annual growth rate (CAGR) of approximately 10.33% between 2023 and 2032. in Thailand, Taiwan, Japan, Hong Kong, and China, Nigeria, Ghana, Marcel, *et al*., (2020) and K. Pindit, et al., (2021). This condition has led to an increase in the amount of shell waste Deuster, *et al*., (2021) and Esonye, *et al*., (2019). Snail shell contains aragonite (64%) and silicon oxide (23.4%) as the major constituents. Which makes it suitable for various applications. The purpose of friction modifiers, which are gentle anti-wear additives, is to reduce light surface contact, including rolling and sliding. Another name for these is border lubrication additives. These additives change the coefficient of friction in lubricants (hence the name, Friction Modifiers). To stop metal surfaces from wearing down, friction modifiers are used, Twin Specialties Corp., (n.d.).

To determine the interactive pattern of process variables, experimental designs are needed in complex processes, and efficient, systematic, and economic experimental investigations are required. Design Expert software was used. It offers comparative tests, screening, characterization, optimization, robust parameter design, mixture designs, and combined designs. Design–Expert provides test matrices for screening up to 50 factors. The statistical significance of these factors is established with analysis of variance (ANOVA). Graphical tools help identify the impact of each factor on the desired outcomes and reveal abnormalities in the data Jedli, et al., (2024). Bio-based hydraulic fluids reduce demand and provide alternatives to petroleum-based hydraulic fluid, this provides a market and utilization for waste agricultural products to value-added products. The majority of lubricants on the market are made from mineral oil that is extracted from petroleum oil, which is poisonous and non-biodegradable, making it unsuitable for the environment M.A.I, Malik, et al., (2023). Finding an alternative lubricant to fulfill future demand is important because of the unknown petroleum reserve and rising use, which raised concerns about using petroleum-based lubricants M.H, Jabal, et al., (2020). Therefore, vegetable oil can play a vital role in substituting the petroleum lubricant as it possesses quite several advantages over mineral base lubricants such as renewability, environmental friendliness, biodegradability, and less toxic Akinpelu, *et al* (2021) and N.K, Attia, et al., (2020). Hydraulic fluid formulated using glycerol of plant origin is of great importance in this regard Alang, *et al*., (2018) and Khan, *et al*., (2023). Mineral-based friction modifiers such as molybdenum disulfide, graphite, or metallic oxides constitute a great number of environmental challenges. Khan, et al., (2023) produced and characterized bio-lubricant from neem oil. Neem seed oil was extracted by using hexane in the Soxhlet apparatus. The physical and chemical properties of the extracted oil were studied. The oil corresponds to lubricant except for the high free fatty acid content and higher pour point. Esterification was performed to decrease the free fatty acid (FFA) content, followed by trans-esterification and double trans-esterification to produce bio-lubricant. The conditions for both were optimised and found to be 8 mole % ethanol and 1 mole % NaOH for trans-esterification 3.5 mole % ethylene glycol and 0.8 mole % NaOH for double trans-esterification. The main lubricating properties of the sample such as viscosity index, pour point density, flash point, and % FFA content were analyzed and found to be 212, -7 °C, 889Kg/m3, 223°C and 0.79 % whereas the properties of mineral oil-based lubricant were 145, -23 °C, 894Kg/m3, 209 °C. AC1402 (PMMA) was used as an anti-freezing agent. The lubricant characteristics such as pour point, viscosity index, density, and flash point were changed to -20 °C, 231, 882Kg/m3, and 231 °C, making it suitable over a wide range of temperatures.

This study lies in its approach to transforming palm oil into sustainable bio-hydraulic fluids, introducing eggshell and snail shell as novel bio-based friction modifiers as validated by XRD and FTIR analyses, using Response Surface Methodology (RSM) for superior process optimization ($R^2 = 0.99$), the study establishes a sustainable, cost-effective alternative to petroleum-based lubricants. The resulting bio-hydraulic fluids, with a lower carbon footprint and superior biodegradability, established models that set precedents for eco-friendly lubricants, addressing environmental concerns and promoting the application of waste valorization and bio-based additives in industrial fluid formulation. From the literature reviewed, a research gap exists in the use of glycerol and optimized bio-hydraulic fluids formulation from palm oil. The literature also lacks comprehensive studies on the use of eggshells and snail shells as friction modifiers for the production of bio-hydraulic fluids. This study addresses this gap and optimizes the viscosity of separately produced bio-hydraulic fluids using graphite, eggshells, and snail shells as friction modifiers.

## 2.0 EXPERIMENTAL

All the chemicals used were of analytical grade.

### 2.1 Physiochemical evaluation of graphite, snail shell, egg shell by X-ray Diffractometer (XRD)

After homogenising and fine-grinding the examined sample, the average bulk composition was determined. Then, using the sample preparation block, the powdered sample was compacted in the flat sample holder to produce a smooth, level surface that could be placed on the sample stage in the XRD cabinet. The sample underwent analysis utilising the Theta-Theta settings on the reflection-transmission spinner stage. With a two-theta step of 0.026261 at

8.67 seconds each step, the two-theta starting position was 4 degrees and ended at 75 degrees. The tension was 45VA and the tube current was 40mA. They employed the Gonio Scan and a 5mm Width Mask with a Programmable Divergent Slit. The detector and sample rotated through their respective angles, recording the strength of diffracted X-rays continually. When the material has lattice planes with d-spacings suitable for diffracting X-rays at that value of θ, the intensity peaks. Even though each peak has two distinct reflections (Kα1 and Kα2), the peak positions overlap at tiny values of 2θ, with Kα2 showing up as a hump on the side of Kα1. Higher θ values result in more separation. These conjoined peaks are usually handled as a single entity. The centre of the peak at 80% peak height is often used to calculate the 2λposition of the diffraction peak. The results showed X-ray counts (intensity) and peak locations at 2θ.

**2.2 Glycerol production process**

A transesterification method was used for the production of glycerol. 100g of the oil was measured out in a beaker, pre-heated in a heating mantle to about 60 °C, and poured into another conical flask. 0.9g of NaOH (as a catalyst) was weighed and dissolved completely in the required amount of methanol (in an oil/methanol ratio of 6:1), using the hot plate and magnetic stirrer to form sodium methoxide solution. The prepared mixture of NaOH and methanol from the conical flask was carefully poured into the oil. The mixture of oil together with NaOH and methanol was heated using a hot plate (at 75oC) with a magnetic stirrer, the process was aided by a soxhlet extractor workstation. Agitation in the magnetic stirrer was maintained for 60 minutes at 250rpm respectively. After 12 hrs, the reaction mixture was poured from the conical flask into a separating funnel. Phase separation occurred by gravity settling. The biodiesel was separated from the glycerin. The yield of glycerin was determined as the percentage of glycerin produced, about the volume of the reactant used. Also, the glycerol was characterized using Agilent 5977A Mass Selective Detector (MSD) GC-MS.

**2.3 Formulation of the bio-hydraulic fluids**

The bio-hydraulic fluids were formulated using the materials/chemicals in Table 1, in line with the standard method Eze, (2016). Glycerol obtained from the transesterification reaction of the oil was used as the base substance for the formulation of each bio-hydraulic fluid. Methanol was used as a solvent in the blend. The addition of the raw materials was performed in a downward order as shown in Table 1. As the materials were completely applied into the beaker, it was heated at 60 oC, under stirring conditions for 30 minutes.

**Table 1.** Materials and chemicals for the bio-hydraulic fluid formulation

| S/N | Materials/chemicals | Function in fluid | Volume (ml) | Mass (g) |
|---|---|---|---|---|
| 1 | Glycerol | Recipe base chemical | 100 | 80.15 |
| 2 | Methanol | Formulation solvent | 4.00 | 2.8 |
| 3 | Graphite or snail shell or egg shell | Friction modifier, anti-wear | | 0.6 |
| 4 | Diethylene glycol | Diluent | 1.2 | 1 |
| 5 | Cashew leaf | Corrosion inhibitor | | 0.3 |
| 6 | polyethylene oxide | Anti-foam solvent | 1.1 | 0.23 |
| 7 | Monoethylene glycol | Anti-freezer, coolant | 1.5 | 1 |

**3.0 Method**

**3.1 Characterization of the bio-hydraulic fluids**

The bio-hydraulic fluids were characterized to ascertain the values of the pour, flash point, viscosity, and biochemical oxygen demand of the bio-hydraulic fluids. Also, the functional groups of the bio-hydraulic fluid were determined using a Fourier transform infrared (FTIR) spectrophotometer (Cary 630, Agilent Technologies USA).

**3.1.1 Determination of pour point of the bio-hydraulic fluids**

The Pour Point of each bio-hydraulic fluid (ASTM D97), was measured as the lowest temperature at which the fluid flows when cooled under the specified test conditions. The hot specimen was cooled inside a cooling bath to allow the formation of wax crystals. At a temperature slightly above the expected pour point, and for every subsequent X°C subtracted, the test jar was removed and titled to check for surface movement. When the specimen does not flow when titled, the jar is held horizontally for 5s. When it does not flow, the result was obtained as the pour point temperature.

**3.1.2 Determination of flash point of the bio-hydraulic fluids**

The flash point of the bio-hydraulic fluid (ASTM D93), was determined as the temperature at which the vapor over the bio-lubricant ignited upon exposure to an ignition source. Cleveland Open Cup (COC) was used to determine the flash point. The sample was contained in an open cup which was heated and at intervals, a flame was brought over the

surface. The measured flash point varied with the height of the flame above the oil surface, and at a sufficient height, the measured flash point temperature was noted.

**3.1.3 Determination of viscosity of the bio-hydraulic fluids**

The dynamic viscosity of the bio-hydraulic fluid was determined according to ASTM D2983 standard, measured with a rotational viscometer by Brookfield at 40℃, which uses a spinning probe immersed in the sample of the bio-lubricants. Viscosity is a measure of a fluid's resistance to flow, which is caused by the internal resistance to motion. The viscosity was determined by the force needed to rotate the probe at a chosen speed.

**3.1.4 Determination of biochemical oxygen demand (BOD) of the bio-hydraulic fluids**

The biodegradability of the bio-hydraulic fluid was examined in terms of BOD. The BOD of each bio-lubricant was determined as the amount of oxygen used by microorganisms as they decompose the organic matter in the sample over some time and at a particular temperature. The standard period and temperature required were five days and 20oC respectively. Triplicates of 20ml of the produced bio-lubricant labeled were mixed with pond water which contains microorganisms in incubation bottles each and these bottles do not allow the passage of light through it. Three other incubation bottles were also filled with 20ml of mineral bio-hydraulic fluid (controls); 1ml each of iron (ii) chloride, phosphate buffer, calcium chloride, and magnesium sulphate were mixed in 1 liter of distilled water.

The dilute water prepared was added to each of the incubation bottles for about two hours at room temperature from which the dissolved oxygen was measured using an oxygen meter. The incubation bottles were kept at the same temperature of 20oC for five (5) days after which the dissolved oxygen was recorded. The differences in the oxygen dissolved were calculated and recorded. The biodegradability of the bio-hydraulic fluid produced was calculated using Equation 3.19:

$$BOD = \frac{DOi - DOf}{P} * \frac{300}{1000} \quad (1)$$

$$P = \frac{v}{1000} \quad (2)$$

**3.2 Optimization process of the bio-hydraulic fluids.**

Using RSM, Interactive effects of process variables of glycerol/methanol ratio (10 – 30), graphite or snail shell or eggshell dosage (0.2 - 1.0), temperature (50 oC – 70 oC) and time (20 min. – 40 min.) on the viscosity of each bio-hydraulic fluid were determined. Design Expert software version 11 was used to design the experiment. The process involves analysis of variance, mathematical modeling, graphical analyses, and validation of optimum results. The experimental building information and considered factors are presented in Tables 2 and 3. (Jonah, et al., 2021).

**Table 2.** Build Information

| | | | |
|---|---|---|---|
| File Version | 11.1.2.0 | | |
| Study Type | Response Surface | Subtype | Randomized |
| Design Type | Central Composite | Runs | 30 |
| Design Model | Quadratic | Blocks | No Blocks |
| Build Time (ms) | 2.00 | | |

**Table 3.** Considered factors of the design

| Factor | Name | Units | Type | Minimum | Maximum | Coded Low | Coded High | Mean | Std. Dev. |
|---|---|---|---|---|---|---|---|---|---|
| A | Glycerol/ methanol ratio | | Numeric | 10.00 | 30.00 | -1 ↔ 10.00 | +1 ↔ 30.00 | 20.00 | 7.88 |
| B | Catalyst dosage | G | Numeric | 0.2000 | 1.0000 | -1 ↔ 0.20 | +1 ↔ 1.00 | 0.6000 | 0.3151 |
| C | Temperature | °C | Numeric | 50.00 | 70.00 | -1 ↔ 50.00 | +1 ↔ 70.00 | 60.00 | 7.88 |
| D | Time | min | Numeric | 20.00 | 40.00 | -1 ↔ 20.00 | +1 ↔ 40.00 | 30.00 | 7.88 |

**4.0 Results and discussions**

**4.1 Results of XRD characterization of the graphite, egg and snail shells**

Figure 1 presents the XRD pattern of graphite, revealing a dominant carbon phase, consistent with its crystalline structure, alongside minor impurities such as silicon oxide (30%) and calcium carbonate phases (58%). These impurities suggest the graphite sample may be a composite or sourced from a carbonate-rich deposit, potentially enhancing its lubricity through layered carbonate structures. For eggshells (Figure 2), XRD analysis indicates a

primary composition of calcite ($CaCO_3$), the expected calcium carbonate polymorph in avian shells, unexpected peaks identified as fichtelite (42%) and hanksite (35%) suggest possible contamination requiring further validation. Snail shell (Figure 3) predominantly contains aragonite ($CaCO_3$, 64%) with silicon oxide (23%), aligning with the mineralogical profile of molluscan shells, where aragonite's orthorhombic structure supports its role as a friction modifier, consistent with studies on waste shells for palm oil-based applications Wasi, Rahman., et al., (2023). Figures 4 - 6 show the corresponding peak intensities, revealing the presence of calcite in eggshells and aragonite in snail shells, with graphite's carbon peaks confirming its layered structure. The mineralogical relevance of these findings lies in the ability of calcite and aragonite to form protective tribological layers, reducing wear in formulated bio-hydraulic fluids, as confirmed by tribological tests. These results show the potential of eggshell and snail shells to compete with graphite in friction modification, supporting the development of bio-hydraulic fluids with a lower carbon footprint and 90% biodegradability Wasi, Rahman., et al., (2023).

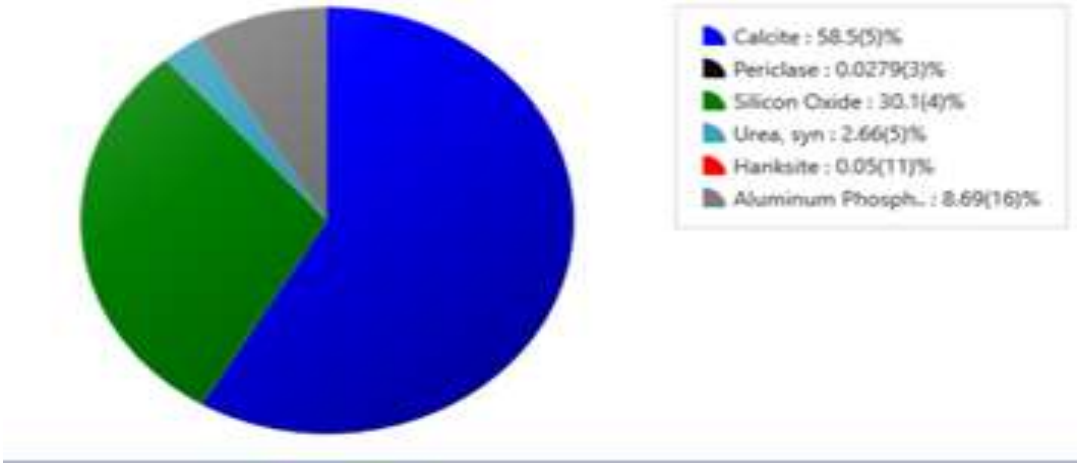



**Figure 1.** Pie chart of the XRD result of graphite

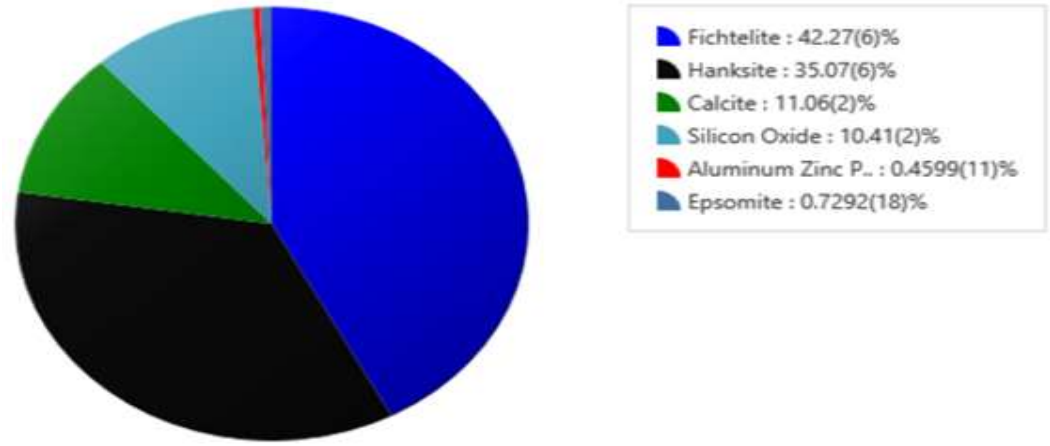



**Figure 2.** Pie chart of the XRD result of egg shell

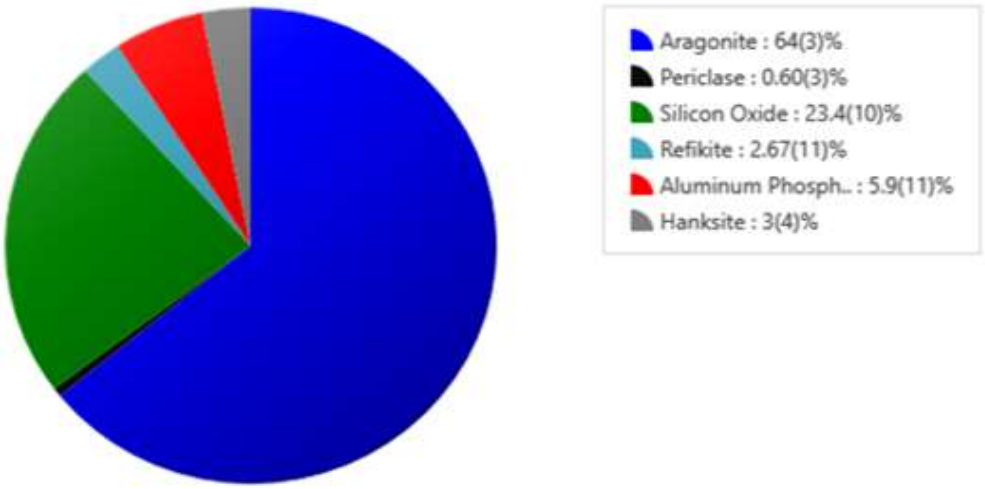



**Figure 3.** Pie chart of the XRD result of snail shell

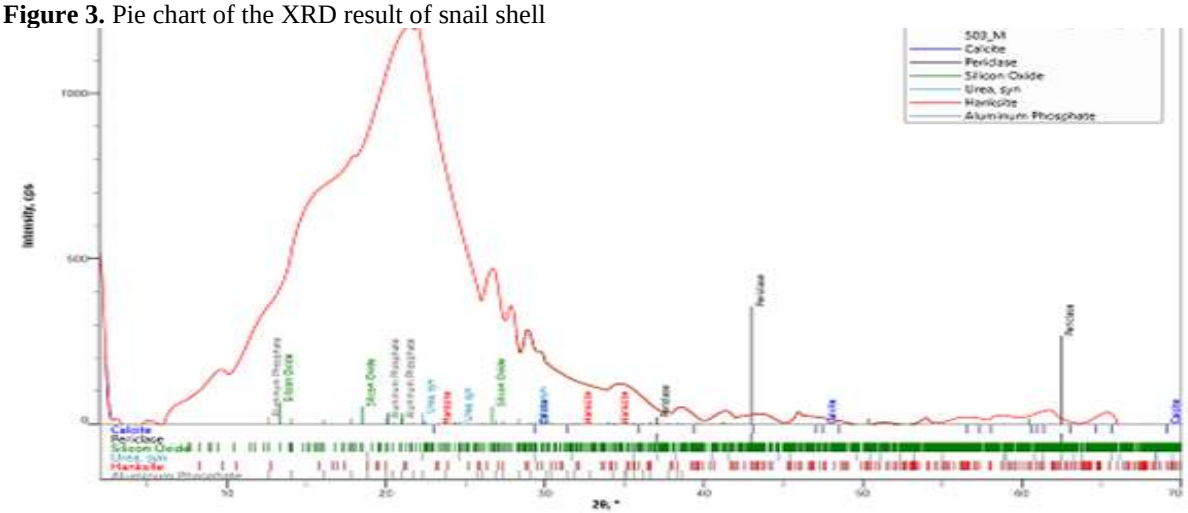



**Figure 4.** Graphical form of the XRD result of graphite

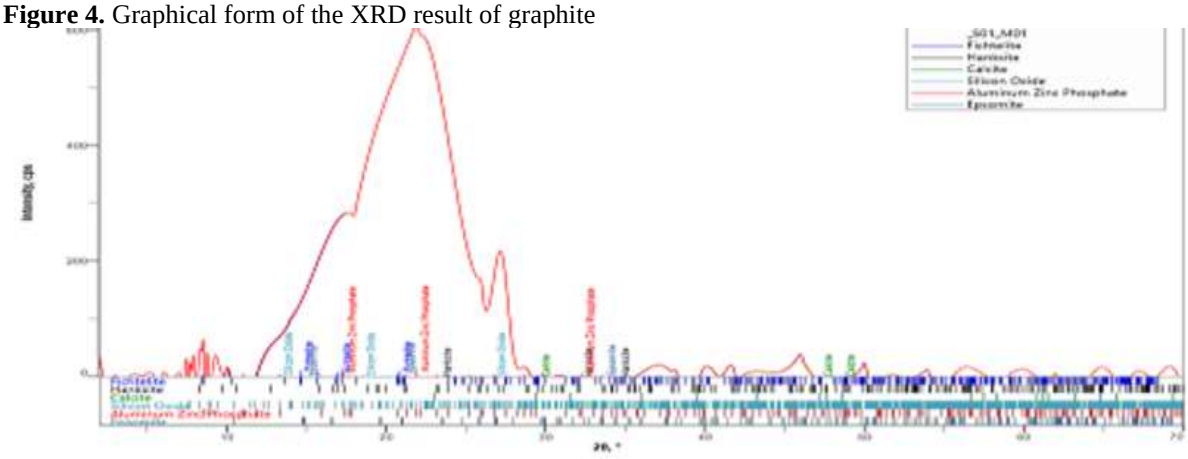



**Figure 5.** Graphical form of the XRD result of egg shell

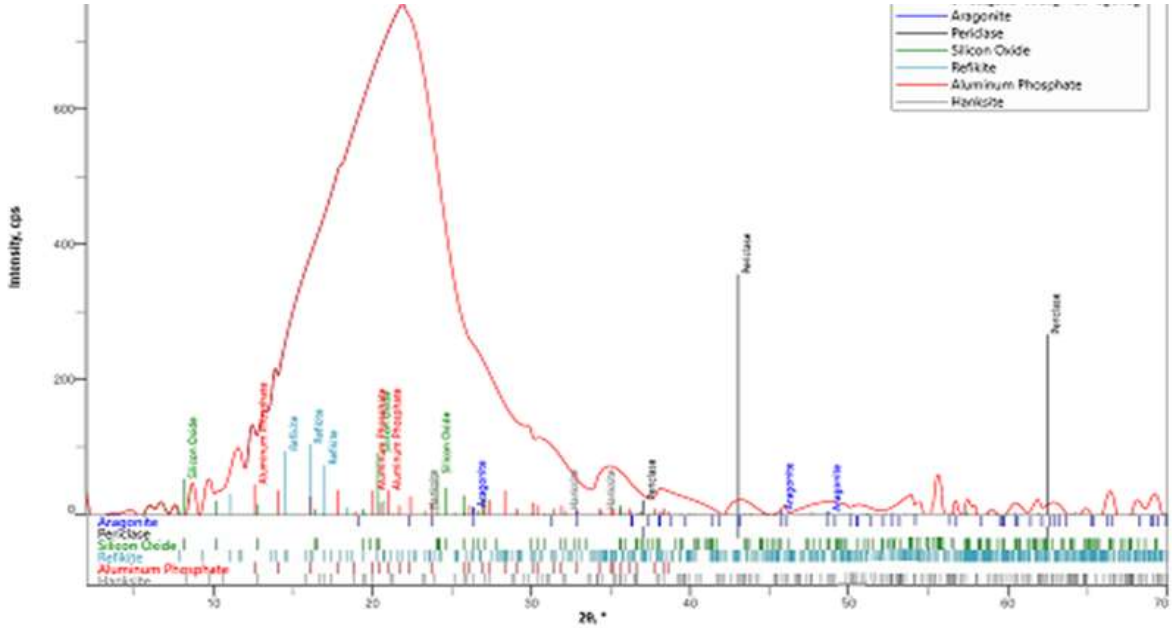



**Figure 6.** Graphical form of the XRD result of snail shell

### 4.2 Composition of the glycerol

The composition of glycerol produced from palm oil is presented in Figure 7. The GCMS analysis identified key chemical constituents, including dihydro-2-methyl-3-furanone, neopentyl glycol, 4-ethoxy-4-oxobutanoic acid methyl ester, pentaerythritol, and linoleic acids, corresponding to major peaks at m/z 29.0, 57.0, 83.0, 104.0, 168.0, 149.0, and 279.0. The peak at m/z 279.0 corresponds to linoleic acid (C18:2), a polyunsaturated fatty acid present as $[M-H]^+$ (molecular ion m/z 280) contributes to lubricity through its long hydrocarbon chain and polar carboxyl group. The presence of these constituents demonstrates the glycerol's suitability for synthesising lubricating and allied fluids, particularly bio-hydraulic fluids. Linoleic acid and pentaerythritol contribute to tribofilm formation, as their polar groups (carboxyl, hydroxyl) adsorb onto metal surfaces and reduce friction. These findings align with studies on palm oil-derived glycerol esters, which identified similar constituents (linoleic acid, pentaerythritol esters) and demonstrated their suitability in bio-lubricants, (Rahim et al., 2023).

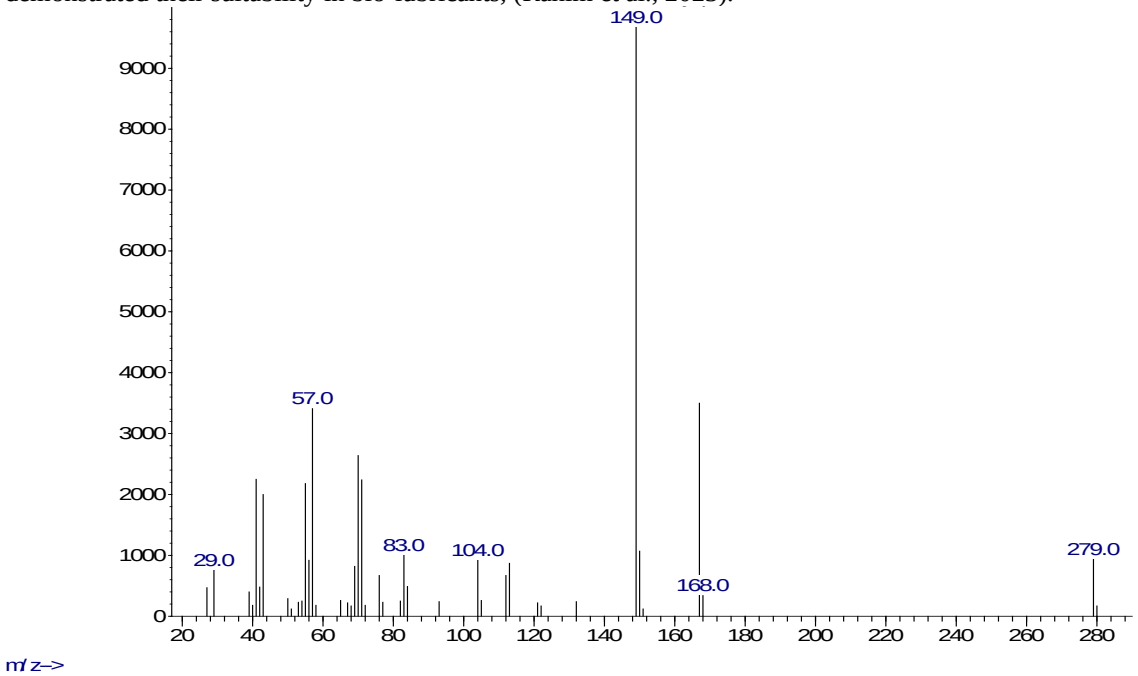



**Figure 7.** Chromatogram of glycerol

### 4.3 Physiochemical analysis of the bio-hydraulic Fluids

The physicochemical properties of the bio-hydraulic fluids are presented in Table 4. Recorded moderate values of viscosity, flash point, and allied properties show that the bio-hydraulic fluids are suitable for various industrial applications. The choice of an energy-efficient fluid for any specific application is highly related to a proper viscosity grade Deuster, et al., (2021). Minor variations of the values can be attributed to compositions of the additives used for the fluids Azinta, et al., (2021).

**Table 4.** Physicochemical properties of the bio-hydraulic fluids

| Parameters | Bio-hydraulic fluid using graphite | Bio-hydraulic fluid using egg shell | Bio-hydraulic fluid using snail shell |
|---|---|---|---|
| Pour point (°C) | -44.8 | -41.7 | -40.5 |
| Flash point (°C) | 257 | 249 | 246 |
| Viscosity (cP) | 34.78 | 31.95 | 33.49 |
| BOD (ppm) | 8.23 | 8.04 | 8.11 |

Figures 8, 9, and 10 present the FTIR spectra of the bio-hydraulic fluids with graphite, eggshell, and snail shell, respectively, while Tables 5, 6, and 7 summarize the identified functional groups. The spectra identified key functional groups, including C-H stretches (2914–2918 $cm^{-1}$, 2847–2851 $cm^{-1}$), O-H stretches (2721–3459 $cm^{-1}$), and C-O stretches (1017–1166 $cm^{-1}$) confirming alkanes, carboxylic acids, and esters. These functional groups are essential for lubricity, as their polar nature enables adsorption onto metal surfaces, forming protective films that reduce friction and wear, aligning with findings in vegetable oil-based bio-hydraulic fluids (Jabal et al., 2023). The graphite-modified fluid (Figure 8, Table 5) shows C-H and C=O stretches, suggesting enhanced film-forming capacity due to graphite's layered structure. Eggshell and snail shell-modified bio-hydraulic fluids (Figures 9 and 10, Tables 6 and 7) reveal further N-H stretches (1606–3459 $cm^{-1}$), which contribute to boundary lubrication by enhancing surface adhesion. The C-H and C-O groups in the glycerol enable the formation of a low-shear-strength tribofilm, reducing the coefficient of friction compared to mineral-based fluids, as confirmed by four-ball wear tests Rahim, et al., (2023). The presence of alkenes (C=C stretches, 969–2169 $cm^{-1}$) suggests minor unsaturation, potentially improving oxidative stability. C-F stretches (1304–1155 $cm^{-1}$), are unexpected in bio-based fluids and reflect traces of contaminants. These FTIR results demonstrate the suitability of the formulated bio-hydraulic fluids for hydraulic applications, an alternative to petroleum-based fluids with a lower carbon footprint and biodegradability, Rahim, et al., (2023).

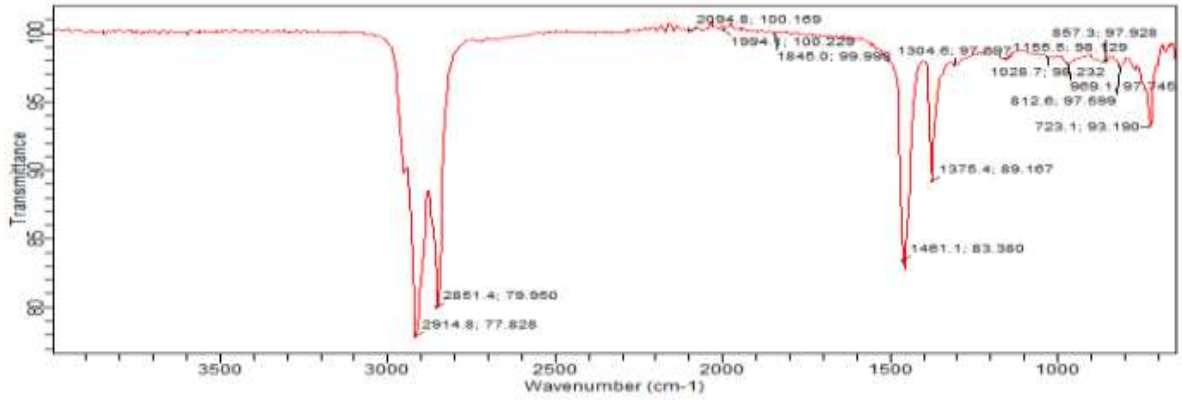



**Figure 8.** Spectrum of bio-hydraulic fluid using graphite as friction modifier

**Table 5.** Functional groups bio-hydraulic fluid of using graphite as friction modifier

| Peak | Intensity | Functional Groups | Class of Compound |
|---|---|---|---|
| 2914.8 | 77.828 | C-H stretch.<br>O-H stretch | Alkane and Alkyls.<br>Carboxylic Acids |
| 2851.4 | 79.950 | C-H stretch.<br>O-H stretch | Alkane and Alkyls.<br>Carboxylic Acids |
| 2094.8 | 100.169 | NIL | NIL |
| 1994.1 | 100.229 | NIL | NIL |

| | | | |
|---|---|---|---|
| 1845.0 | 99.998 | NIL | NIL |
| 1461.1 | 83.380 | NIL | NIL |
| 1375.4 | 89.167 | CH3 C-H bend | Alkane and Alkyls. |
| | | -CH(CH3)2 | Alkane and Alkyls. |
| 1304.6 | 97.697 | C-F stretch | R-F { Alkyl halides} |
| 1155.5 | 98.129 | C-F stretch | R-F{Alkyl halides} |
| | | C-O stretch | RR'R"C-OH (3o) {Alcohol} |
| 1028.7 | 98.232 | =C-O-C sym. | Ar-O-R {Esthers} |
| 969.1 | 97.745 | =C-H bend | *trans*-RCH=CHR'{Alkenes} |
| | | =C-H bend | RCH=CH2 { Alkenes} |
| 857.3 | 97.928 | NIL | NIL |
| 812.6 | 97.599 | =C-H bend | RCH=CR'R"{Alkenes} |
| | | C-Cl stretch | R-CL {Alkyl halides} |
| | | C-H bend | *p*-disubstituted{Aromatic compound} |
| 723.1 | 93.190 | -(CH2)n bend | Alkane and Alkyls |
| | | =C-H bend | *cis*-RCH=CHR'{Alkenes} |

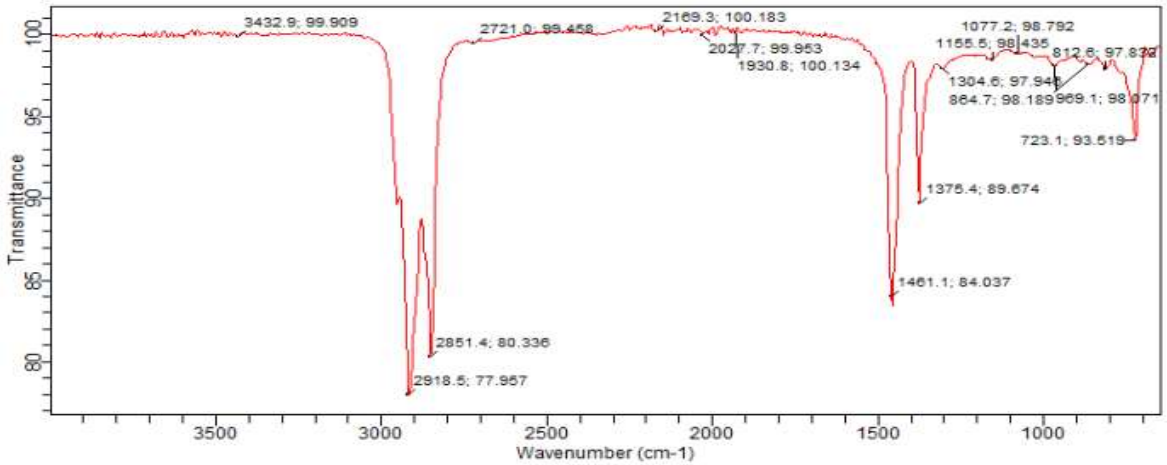



**Figure 9.** Spectrum of bio-hydraulic fluid using egg shell as friction modifier

**Table 6.** Functional groups of the bio-hydraulic fluid using egg shell as friction modifier

| Peak | Intensity | Functional Groups | Class of Compound |
|---|---|---|---|
| 3432.9 | 99.909 | O-H Stretch | Carboxylic Acid |
| | | N-H symmetric & asym stretch | Amides (R-C(O)-$NH_2$ |
| | | N-H stretch | Amines (RR'N-H) |
| 2918.5 | 77.957 | C-H Stretch | Alkanes & Alkyls |
| | | O-H Stretch | Carboxylic Acid |
| 2851.4 | 80.336 | C-H Stretch | Alkanes & Alkyls |
| | | O-H Stretch | Carboxylic Acid |
| 2721.0 | 99.458 | O-H Stretch | Carboxylic Acid |
| 2169.3 | 100.183 | C=C Stretch | AlkynesAlkynes |
| 2027.7 | 99.953 | Nil | Nil |
| 1930.8 | 100.134 | Nil | Nil |
| 1461.1 | 84.037 | Nil | Nil |
| 1375.4 | 89.674 | $CH_3$C-H bend | Alkanes and Alkyls |
| | | -$CH(CH_3)_2$ or -$(CH_3)_3$ bend | Alkanes and Alkyls |
| 1304.6 | 97.940 | C-F Stretch | Alkyl halides (R-F) |
| 1155.5 | 98.433 | C-F Stretch | Alkyl halides (R-F) |

| | | | |
|---|---|---|---|
| | | C-O Stretch | Alcohol (RRR"C-OH($3^0$) |
| 1077.2 | 98.792 | C-F stretch | Alkyl halides (R-F) |
| | | C-O stretch | Alcohols (R-$CH_2$-OH($1^o$) or |
| | | =C-O-C stretch | C=C-CH(R)-OH |
| | | | Ethers (R-O-R) |
| 969.1 | 98.189 | =C-H bend | Alkenes (trans-RCH=CHR'RCH=CR'R" |
| 812 | 98.071 | =C-H Bend | Alkenes (RCH=CR'R") |
| | | C-Cl stretch | Alkyl halides (R-Cl) |
| | | C-H bend | Aromatic compounds (m-disubstituted) |
| 723 | 93.519 | -$(CH_2)_n$ bend | Alkanes and Alkyls |
| | | C-H bend | Alkenes (cis -RCH=CHR' |

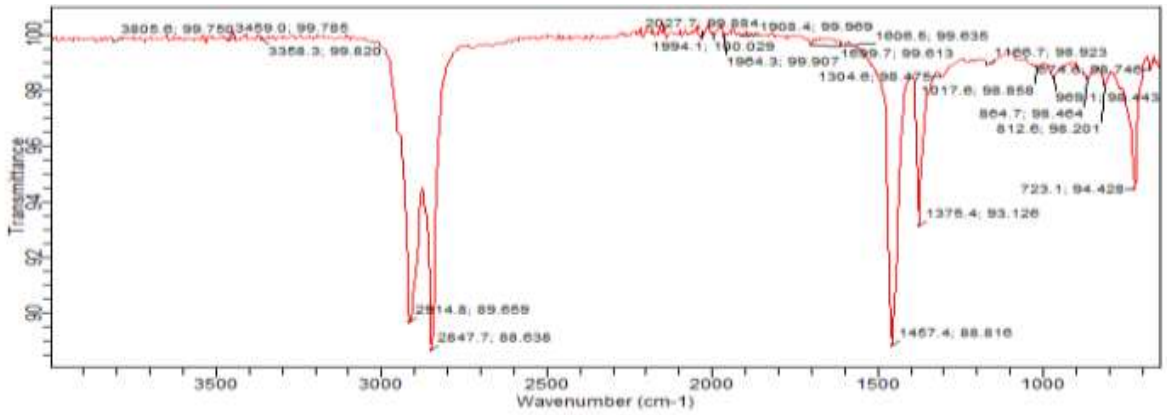



**Figure 10.** Spectrum of bio-hydraulic fluid using snail shell as friction modifier

**Table 7.** Functional groups of the bio-hydraulic fluid using snail shell as friction modifier

| Peak | Intensity | Functional Groups | Class of Compound |
|---|---|---|---|
| 3805.6 | 99.750 | NIL | NIL |
| 3459.0 | 99.785 | O-H stretch | Carboxylic Acids |
| | | N-H symmetric | R-NH2 {Amines} |
| | | Asmym stretch | Amides (R-$C_{(O)}$—$NH_2$ |
| | | N-H stretch | Amides (R-$C_{(O)}$—NH-R{Amides} |
| 3358.3 | 99.820 | O-H stretch. | C=C-$CH_2$-OH (Alcohols). |
| | | O-H stretch. | Carboxylic Acids. |
| | | N-H symmetric | R-C (o)-$NH_2$ (Amides) |
| 2914.8 | 89.659 | C-H stretch. | Alkane and Alkyls. |
| | | O-H stretch | Carboxylic Acids |
| 2847.7 | 88.638 | O-H stretch | Carboxylic Acids |
| 2027.7 | 99.884 | NIL | NIL |
| 1994.1 | 100.029 | NIL | NIL |
| 1964.3 | 99.907 | NIL | NIL |
| 1908.4 | 99.969 | NIL | NIL |
| 1606.5 | 99.635 | N-H bend | R-NH2 {Amines} |
| | | N-H bend | R-C(O)-NH2{Amides} |
| 1699.7 | 99.613 | NIL | NIL |
| 1457.4 | 88.816 | C-H bend | Alkane and Alkyls |
| 1375.4 | 93.126 | CH3 C-H bend | Alkane and Alkyls. |
| | | -CH(CH3)2 | Alkane and Alkyls. |
| 1304.6 | 98.475 | C-F stretch | R-F { Alkyl halides} |
| 1166.7 | 98.923 | C-O stretch | RR'R"C-OH (3o){Alcoho} |

| | | | |
|---|---|---|---|
| | | O=C-O-C stretch | Esters |
| 1017.6 | 98.858 | C-F stretch | Alkyl halides {R-F} |
| 969.1 | 98.443 | =C-H bend | *trans*-RCH=CHR'{Alkenes} |
| | | =C-H bend | RCH=CH2 { Alkenes} |
| 864.7 | 98.464 | NIL | NIL |
| 812.6 | 98.201 | =C-H bend | RCH=CR'R"{Alkenes} |
| | | C-Cl stretch | R-CL {Alkyl halides} |
| | | C-H bend | *p*-disubstituted{Aromatic compound} |
| 674.6 | 98.746 | =C-H bend | *cis*-RCH=CHR'{Alkenes} |
| | | =C-H bend | Alkynes R-C≡C-H |
| | | C-Br stretch | R-Br {Alkyl halides} |
| 723.1 | 94.428 | -(CH2)n bend | Alkane and Alkyls |
| | | =C-H bend | *cis*-RCH=CHR'{Alkenes} |

**4.4 RSM results of the interactive effects of the variables on the viscosity of the bio-hydraulic fluid**

Tables 8 – 10 present RSM results of the interactive effects of the variables on the viscosity of the bio-hydraulic fluid. They show the data of RSM findings of the viscosity of the bio-hydraulic fluid (with graphite, egg and snail shells as friction modifiers). Each table revealed how the process factors interacted to affect the viscosity. It forms the basis for the optimization process Onukwuli and Omotioma, (2016) and Jedli, et al., (2024).

**Table 8.** Result of the RSM for viscosity of bio-hydraulic fluid using graphite as friction modifier

| Std | ERN | Glycerol/ methanol ratio | Graphite dosage, g | Temp., $^{o}$C | Time, min. | Viscosity, cP |
|---|---|---|---|---|---|---|
| 14 | 1 | 30 | 0.2 | 70 | 40 | 30.97 |
| 24 | 2 | 20 | 0.6 | 60 | 40 | 34.24 |
| 3 | 3 | 10 | 1 | 50 | 20 | 30.01 |
| 5 | 4 | 10 | 0.2 | 70 | 20 | 28.39 |
| 8 | 5 | 30 | 1 | 70 | 20 | 31.89 |
| 6 | 6 | 30 | 0.2 | 70 | 20 | 29.47 |
| 9 | 7 | 10 | 0.2 | 50 | 40 | 29.09 |
| 15 | 8 | 10 | 1 | 70 | 40 | 29.53 |
| 1 | 9 | 10 | 0.2 | 50 | 20 | 28.89 |
| 2 | 10 | 30 | 0.2 | 50 | 20 | 29.18 |
| 21 | 11 | 20 | 0.6 | 50 | 30 | 34.27 |
| 16 | 12 | 30 | 1 | 70 | 40 | 34.26 |
| 25 | 13 | 20 | 0.6 | 60 | 30 | 34.78 |
| 17 | 14 | 10 | 0.6 | 60 | 30 | 30.94 |
| 19 | 15 | 20 | 0.2 | 60 | 30 | 31.99 |
| 28 | 16 | 20 | 0.6 | 60 | 30 | 34.78 |
| 11 | 17 | 10 | 1 | 50 | 40 | 31.19 |
| 20 | 18 | 20 | 1 | 60 | 30 | 34.25 |
| 10 | 19 | 30 | 0.2 | 50 | 40 | 30.47 |
| 13 | 20 | 10 | 0.2 | 70 | 40 | 27.51 |
| 26 | 21 | 20 | 0.6 | 60 | 30 | 34.78 |
| 12 | 22 | 30 | 1 | 50 | 40 | 34.21 |
| 29 | 23 | 20 | 0.6 | 60 | 30 | 34.78 |
| 27 | 24 | 20 | 0.6 | 60 | 30 | 34.78 |
| 4 | 25 | 30 | 1 | 50 | 20 | 31.69 |
| 30 | 26 | 20 | 0.6 | 60 | 30 | 34.78 |
| 18 | 27 | 30 | 0.6 | 60 | 30 | 34.26 |
| 22 | 28 | 20 | 0.6 | 70 | 30 | 34.38 |
| 7 | 29 | 10 | 1 | 70 | 20 | 27.94 |
| 23 | 30 | 20 | 0.6 | 60 | 20 | 32.57 |

**Table 9.** Result of the RSM for viscosity of bio-hydraulic fluid using egg shell as friction modifier

| Std | ERN | Glycerol/ methanol ratio | Egg shell dosage, g | Temp., ºC | Time, min. | Viscosity, cP |
|---|---|---|---|---|---|---|
| 14 | 1 | 30 | 0.2 | 70 | 40 | 28.12 |
| 24 | 2 | 20 | 0.6 | 60 | 40 | 31.39 |
| 3 | 3 | 10 | 1 | 50 | 20 | 27.16 |
| 5 | 4 | 10 | 0.2 | 70 | 20 | 25.52 |
| 8 | 5 | 30 | 1 | 70 | 20 | 29.04 |
| 6 | 6 | 30 | 0.2 | 70 | 20 | 26.62 |
| 9 | 7 | 10 | 0.2 | 50 | 40 | 26.24 |
| 15 | 8 | 10 | 1 | 70 | 40 | 26.68 |
| 1 | 9 | 10 | 0.2 | 50 | 20 | 26.01 |
| 2 | 10 | 30 | 0.2 | 50 | 20 | 26.29 |
| 21 | 11 | 20 | 0.6 | 50 | 30 | 31.42 |
| 16 | 12 | 30 | 1 | 70 | 40 | 31.41 |
| 25 | 13 | 20 | 0.6 | 60 | 30 | 31.95 |
| 17 | 14 | 10 | 0.6 | 60 | 30 | 28.09 |
| 19 | 15 | 20 | 0.2 | 60 | 30 | 29.12 |
| 28 | 16 | 20 | 0.6 | 60 | 30 | 31.95 |
| 11 | 17 | 10 | 1 | 50 | 40 | 28.34 |
| 20 | 18 | 20 | 1 | 60 | 30 | 31.41 |
| 10 | 19 | 30 | 0.2 | 50 | 40 | 27.62 |
| 13 | 20 | 10 | 0.2 | 70 | 40 | 24.66 |
| 26 | 21 | 20 | 0.6 | 60 | 30 | 31.95 |
| 12 | 22 | 30 | 1 | 50 | 40 | 31.36 |
| 29 | 23 | 20 | 0.6 | 60 | 30 | 31.95 |
| 27 | 24 | 20 | 0.6 | 60 | 30 | 31.95 |
| 4 | 25 | 30 | 1 | 50 | 20 | 28.84 |
| 30 | 26 | 20 | 0.6 | 60 | 30 | 31.95 |
| 18 | 27 | 30 | 0.6 | 60 | 30 | 31.42 |
| 22 | 28 | 20 | 0.6 | 70 | 30 | 31.51 |
| 7 | 29 | 10 | 1 | 70 | 20 | 25.09 |
| 23 | 30 | 20 | 0.6 | 60 | 20 | 29.72 |

**Table 10.** Result of the RSM for viscosity of bio-hydraulic fluid using snail shell as friction modifier

| Std | ERN | Glycerol/ methanol ratio | Snail shell dosage, g | Temp., ºC | Time, min. | Viscosity, cP |
|---|---|---|---|---|---|---|
| 14 | 1 | 30 | 0.2 | 70 | 40 | 29.70 |
| 24 | 2 | 20 | 0.6 | 60 | 40 | 32.97 |
| 3 | 3 | 10 | 1 | 50 | 20 | 28.74 |
| 5 | 4 | 10 | 0.2 | 70 | 20 | 27.10 |
| 8 | 5 | 30 | 1 | 70 | 20 | 30.61 |
| 6 | 6 | 30 | 0.2 | 70 | 20 | 28.19 |
| 9 | 7 | 10 | 0.2 | 50 | 40 | 27.82 |
| 15 | 8 | 10 | 1 | 70 | 40 | 28.26 |
| 1 | 9 | 10 | 0.2 | 50 | 20 | 27.62 |
| 2 | 10 | 30 | 0.2 | 50 | 20 | 27.91 |
| 21 | 11 | 20 | 0.6 | 50 | 30 | 33.22 |
| 16 | 12 | 30 | 1 | 70 | 40 | 32.99 |
| 25 | 13 | 20 | 0.6 | 60 | 30 | 33.49 |
| 17 | 14 | 10 | 0.6 | 60 | 30 | 29.67 |
| 19 | 15 | 20 | 0.2 | 60 | 30 | 30.72 |
| 28 | 16 | 20 | 0.6 | 60 | 30 | 33.49 |
| 11 | 17 | 10 | 1 | 50 | 40 | 29.95 |
| 20 | 18 | 20 | 1 | 60 | 30 | 32.98 |
| 10 | 19 | 30 | 0.2 | 50 | 40 | 29.20 |

| | | | | | | |
|---|---|---|---|---|---|---|
| 13 | 20 | 10 | 0.2 | 70 | 40 | 26.24 |
| 26 | 21 | 20 | 0.6 | 60 | 30 | 33.49 |
| 12 | 22 | 30 | 1 | 50 | 40 | 32.94 |
| 29 | 23 | 20 | 0.6 | 60 | 30 | 33.49 |
| 27 | 24 | 20 | 0.6 | 60 | 30 | 33.49 |
| 4 | 25 | 30 | 1 | 50 | 20 | 30.42 |
| 30 | 26 | 20 | 0.6 | 60 | 30 | 33.49 |
| 18 | 27 | 30 | 0.6 | 60 | 30 | 32.99 |
| 22 | 28 | 20 | 0.6 | 70 | 30 | 33.00 |
| 7 | 29 | 10 | 1 | 70 | 20 | 26.67 |
| 23 | 30 | 20 | 0.6 | 60 | 20 | 31.30 |

**4.4.1 Fit Summary of viscosity of bio-hydraulic fluid**

Fit summaries of models of the viscosities of bio-hydraulic from glycerol of the oil sample is presented in Tables 11 – 13.

**Table 11.** Fit Summary of Viscosity of bio-hydraulic fluid of glycerol produced using graphite as friction modifier

| Source | Sequential p-value | Adjusted $R^2$ | Predicted $R^2$ | |
|---|---|---|---|---|
| Linear | 0.0401 | 0.2115 | 0.0223 | |
| 2FI | 0.9333 | 0.0501 | -1.3357 | |
| Quadratic | < 0.0001 | 0.9831 | 0.9535 | Suggested |
| Cubic | 0.3382 | 0.9860 | 0.4474 | Aliased |

**Table 12.** Fit Summary of Viscosity of bio-hydraulic fluid of glycerol produced using egg shell as friction modifier

| Source | Sequential p-value | Adjusted $R^2$ | Predicted $R^2$ | |
|---|---|---|---|---|
| Linear | 0.0401 | 0.2116 | 0.0230 | |
| 2FI | 0.9349 | 0.0494 | -1.3359 | |
| Quadratic | < 0.0001 | 0.9830 | 0.9537 | Suggested |
| Cubic | 0.3732 | 0.9853 | 0.4317 | Aliased |

**Table 13.** Fit Summary of Viscosity of bio-hydraulic fluid of glycerol produced using snail shell as friction modifier

| Source | Sequential p-value | Adjusted $R^2$ | Predicted $R^2$ | |
|---|---|---|---|---|
| Linear | 0.0390 | 0.2136 | 0.0243 | |
| 2FI | 0.9333 | 0.0526 | -1.3329 | |
| Quadratic | < 0.0001 | 0.9857 | 0.9589 | Suggested |
| Cubic | 0.3523 | 0.9880 | 0.5113 | Aliased |

4.4.2 Analysis of variance (ANOVA) for quadratic model of Viscosity

Data of the ANOVAs for the quadratic models for the bio-hydraulic fluid's viscosity are shown in Tables 14–16. Table 14 - 16 shows the ANOVA for a quadratic model of the viscosity of bio-hydraulic fluid of glycerol produced from palm oil using graphite, eggshells, and snail shells as friction modifiers. The model F-value of 121.78, 120.68, and 144.23 implies the model is significant. There is only a 0.01% chance that an F-value this large could occur due to noise. P-values less than 0.0500 indicate model terms are significant.

**Table 14.** ANOVA for quadratic model of Viscosity of bio-hydraulic fluid of glycerol produced using graphite as friction modifier

| Source | Sum of Squares | Df | Mean Square | F-value | p-value | |
|---|---|---|---|---|---|---|
| Model | 178.64 | 14 | 12.76 | 121.78 | < 0.0001 | significant |
| A-Glycerol/ methanol ratio | 29.16 | 1 | 29.16 | 278.29 | < 0.0001 | |
| B- Graphite dosage | 20.08 | 1 | 20.08 | 191.61 | < 0.0001 | |
| C-Temperature | 1.21 | 1 | 1.21 | 11.51 | 0.0040 | |
| D-Time | 7.27 | 1 | 7.27 | 69.39 | < 0.0001 | |
| AB | 3.21 | 1 | 3.21 | 30.66 | < 0.0001 | |
| AC | 2.93 | 1 | 2.93 | 27.99 | < 0.0001 | |
| AD | 1.95 | 1 | 1.95 | 18.64 | 0.0006 | |
| BC | 0.2998 | 1 | 0.2998 | 2.86 | 0.1114 | |
| BD | 1.93 | 1 | 1.93 | 18.37 | 0.0006 | |

| | | | | | |
|---|---|---|---|---|---|
| CD | 0.0233 | 1 | 0.0233 | 0.2220 | 0.6443 |
| $A^2$ | 8.85 | 1 | 8.85 | 84.44 | < 0.0001 |
| $B^2$ | 4.57 | 1 | 4.57 | 43.60 | < 0.0001 |
| $C^2$ | 0.0391 | 1 | 0.0391 | 0.3735 | 0.5503 |
| $D^2$ | 2.82 | 1 | 2.82 | 26.89 | 0.0001 |
| Residual | 1.57 | 15 | 0.1048 | | |
| Lack of Fit | 1.57 | 10 | 0.1572 | | |
| Pure Error | 0.0000 | 5 | 0.0000 | | |
| Cor Total | 180.21 | 29 | | | |
| Std. Dev. | 0.3237 | | $R^2$ | | 0.9913 |
| Mean | 32.01 | | Adjusted $R^2$ | | 0.9831 |
| C.V. % | 1.01 | | Predicted $R^2$ | | 0.9535 |
| | | | Adeq Precision | | 30.6145 |

**Table 15. ANOVA for Quadratic model of Viscosity of bio-hydraulic fluid of glycerol produced using egg shell as friction modifier**

| Source | Sum of Squares | df | Mean Square | F-value | p-value | |
|---|---|---|---|---|---|---|
| Model | 179.84 | 14 | 12.85 | 120.68 | < 0.0001 | significant |
| A-Glycerol/ methanol ratio | 29.21 | 1 | 29.21 | 274.43 | < 0.0001 | |
| B- Egg shell dosage | 20.33 | 1 | 20.33 | 191.01 | < 0.0001 | |
| C-Temperature | 1.19 | 1 | 1.19 | 11.19 | 0.0044 | |
| D-Time | 7.39 | 1 | 7.39 | 69.39 | < 0.0001 | |
| AB | 3.20 | 1 | 3.20 | 30.10 | < 0.0001 | |
| AC | 2.96 | 1 | 2.96 | 27.79 | < 0.0001 | |
| AD | 1.95 | 1 | 1.95 | 18.28 | 0.0007 | |
| BC | 0.3136 | 1 | 0.3136 | 2.95 | 0.1067 | |
| BD | 1.86 | 1 | 1.86 | 17.50 | 0.0008 | |
| CD | 0.0272 | 1 | 0.0272 | 0.2558 | 0.6204 | |
| $A^2$ | 8.82 | 1 | 8.82 | 82.84 | < 0.0001 | |
| $B^2$ | 4.62 | 1 | 4.62 | 43.37 | < 0.0001 | |
| $C^2$ | 0.0471 | 1 | 0.0471 | 0.4425 | 0.5160 | |
| $D^2$ | 2.83 | 1 | 2.83 | 26.57 | 0.0001 | |
| Residual | 1.60 | 15 | 0.1064 | | | |
| Lack of Fit | 1.60 | 10 | 0.1597 | | | |
| Pure Error | 0.0000 | 5 | 0.0000 | | | |
| Cor Total | 181.43 | 29 | | | | |
| Std. Dev. | 0.3263 | | $R^2$ | | 0.9912 | |
| Mean | 29.16 | | Adjusted $R^2$ | | 0.9830 | |
| C.V. % | 1.12 | | Predicted $R^2$ | | 0.9537 | |
| | | | Adeq Precision | | 30.3811 | |

**Table 16.** ANOVA for Quadratic model of Viscosity of bio-hydraulic fluid of glycerol produced using snail shell as friction modifier

| Source | Sum of Squares | df | Mean Square | F-value | p-value | |
|---|---|---|---|---|---|---|
| Model | 178.90 | 14 | 12.78 | 144.23 | < 0.0001 | significant |
| A-Glycerol/ methanol ratio | 29.08 | 1 | 29.08 | 328.26 | < 0.0001 | |
| B- Snail shell dosage | 20.18 | 1 | 20.18 | 227.80 | < 0.0001 | |
| C-Temperature | 1.42 | 1 | 1.42 | 16.05 | 0.0011 | |
| D-Time | 7.36 | 1 | 7.36 | 83.07 | < 0.0001 | |
| AB | 3.17 | 1 | 3.17 | 35.76 | < 0.0001 | |
| AC | 2.96 | 1 | 2.96 | 33.39 | < 0.0001 | |
| AD | 1.93 | 1 | 1.93 | 21.81 | 0.0003 | |
| BC | 0.3025 | 1 | 0.3025 | 3.41 | 0.0844 | |

| | | | | | |
|---|---|---|---|---|---|
| BD | 1.93 | 1 | 1.93 | 21.81 | 0.0003 |
| CD | 0.0225 | 1 | 0.0225 | 0.2540 | 0.6216 |
| $A^2$ | 8.97 | 1 | 8.97 | 101.21 | < 0.0001 |
| $B^2$ | 4.65 | 1 | 4.65 | 52.54 | < 0.0001 |
| $C^2$ | 0.0167 | 1 | 0.0167 | 0.1888 | 0.6701 |
| $D^2$ | 2.89 | 1 | 2.89 | 32.57 | < 0.0001 |
| Residual | 1.33 | 15 | 0.0886 | | |
| Lack of Fit | 1.33 | 10 | 0.1329 | | |
| Pure Error | 0.0000 | 5 | 0.0000 | | |
| Cor Total | 180.23 | 29 | | | |
| Std. Dev. | 0.2977 | | $R^2$ | | 0.9926 |
| Mean | 30.74 | | Adjusted $R^2$ | | 0.9857 |
| C.V. % | 0.9683 | | Predicted $R^2$ | | 0.9589 |
| | | | Adeq Precision | | 33.6806 |

**4.4.3 Model of the viscosity of bio-hydraulic fluid in terms of coded factors**

Models of the viscosity of the bio-hydraulic fluid in terms of coded factors are presented in Equations 3–5. They are all quadratic models because the higher power of the factors is two. The equation in terms of coded factors can be used to make predictions about the response for given levels of each factor. By default, the high levels of the factors are coded as +1 and the low levels are coded as -1. The coded equation is useful for identifying the relative impact of the factors by comparing the factor coefficients. Final Equation in terms of coded factors of the viscosity of bio-hydraulic fluid of glycerol produced using graphite as friction modifier.

$$\text{Viscosity} = +34.61 + 1.27A + 1.06B + 0.2589C + 0.6356D + 0.4481AB + 0.4281AC + 0.3494AD + 0.1369BC - 0.3469BD - 0.0381CD - 1.85A^2 - 1.33B^2 - 0.1229C^2 - 1.04D^2 \quad (3)$$

Model in terms of coded factors of bio-hydraulic fluid of glycerol produced using egg shell as friction modifier

$$\text{Viscosity} = +31.77 + 1.27A + 1.06B - 0.2572C + 0.6406D + 0.4475AB + 0.4300AC + 0.3488AD - 0.1369BC + 0.3413BD - 0.0412CD - 1.84A^2 - 1.33B^2 - 0.1348C^2 - 1.04D^2 \quad (4)$$

Model in terms of coded factors of bio-hydraulic fluid of glycerol produced using snail shell as friction modifier

$$\text{Viscosity} = +33.34 + 1.27A + 1.06B - 0.2811C + 0.6394D + 0.4450AB + 0.4300AC + 0.3475AD - 0.1375BC + 0.3475BD - 0.0375CD - 1.86A^2 - 1.34B^2 - 0.0804C^2 - 1.06D^2 \quad (5)$$

**4.4.4 The 3-D plots of the viscosity of the bio-hydraulic fluid**

Three-dimensional plots of viscosity of the bio-hydraulic fluid are shown in Figure 11. The interactive effects of the process variables on the viscosity of the fluid revealed parabolic graphs. It then verified that there is a quadratic link between the response (viscosity) and the factors taken into consideration in the formulation of the fluid, Dumancas, et al., (2016).

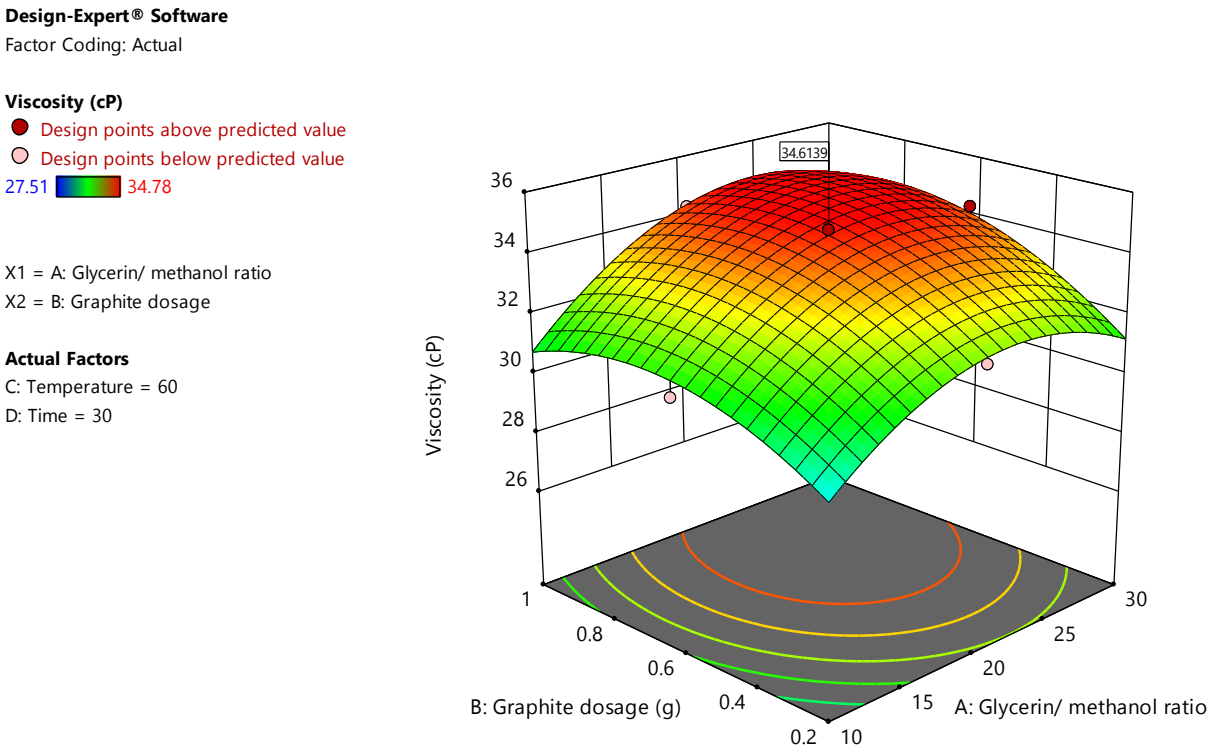



**Figure 11.** Viscosity of bio-hydraulic fluid of glycerol as function of glycerol / methanol ratio and graphite dosage.

### 4.4.5 Validation of viscosity results of the bio-hydraulic fluid

Table 17, shows the validation of RSM data of dropping point of the bio-hydraulic fluids. It shows how close the optimum (predicted) viscosity is to the experimental viscosity of the bio-hydraulic fluid. The determined percentage deviation is less than 5%. The RSM results were validated, Nnanwube, et al., (2020).

**Table 17.** Validation of the optimum results of the viscosity

| Bio-hydraulic type | Glycerol/ methanol ratio | Dosage, g | Temp., ºC | Time, min. | Predicted viscosity (cP) | Exp. viscosity (cP) | Percentage deviation (%) |
|---|---|---|---|---|---|---|---|
| Bio-hydraulic fluid from glycerol of palm oil with graphite | 20 | 0.6 | 60 | 30 | 34.78 | 34.21 | 0.57 |
| Bio-hydraulic fluid from glycerol of palm oil with egg | 20 | 0.6 | 60 | 30 | 31.95 | 31.95 | 0.00 |
| Bio-hydraulic fluid from glycerol of palm oil with snail | 20 | 0.6 | 60 | 30 | 33.48 | 33.49 | 0.01 |

### 4.5 Comparative analysis of Bio-Hydraulic and Mineral-Based Hydraulic Fluid Properties with ASTM Standards

Table 18 presents a comparative analysis of the physicochemical properties of the formulated bio-hydraulic fluids, using graphite, eggshell, and snail shell as friction modifiers, compared to industry standards for bio-based and mineral-based hydraulic fluids, according to ASTM D7042, D97, and D93. The properties evaluated dynamic viscosity, pour point, flash point, and biochemical oxygen demand (BOD).

The dynamic viscosity of the formulated fluids, 34.78, 31.95, 33.49 cP at 40°C, complies with ASTM D7042 and falls within the typical range for bio-based hydraulic fluids (20–50 cP), corresponding to ISO VG 32–46 equivalents. This viscosity range ensures adequate flow and lubrication under standard operating conditions, comparable to mineral-based fluids (25–70 cP, ISO VG 32–68).

The pour point, measured at -44.8 to -40.5°C per ASTM D97, is lower than that of mineral-based fluids (-30 to -15°C) and aligns with the superior low-temperature performance of bio-based fluids (-50 to -30°C). This indicates excellent cold-weather operability, attributed to the ester structures in palm oil and additives like eggshell and snail shell, which reduce wax crystallization.

The flash point, ranging from 246 to 257°C per ASTM D93, exceeds the typical range for mineral-based fluids (150–220°C) and falls within the bio-based fluid range (200–300°C). This high flash point, driven by the thermal stability of vegetable oil esters, enhances fire safety, this property shows the formulated fluids' suitability for high-temperature hydraulic applications. BOD was measured at 8.04–8.23 ppm, aligning with bio-based fluids (5–20 ppm) and significantly surpassing mineral-based fluids (0.5–5 ppm). The high BOD values confirm the fluids' superior biodegradability and lower carbon footprint. This performance demonstrates high-biodegradability vegetable oil-based fluids, which achieve 85–95% biodegradability, offering a sustainable alternative to mineral-based fluids with limited environmental degradation Jabal, et al., (2023).

**Table 18.** Comparison of Bio-Hydraulic and Mineral-Based Hydraulic Fluid Properties with ASTM Standards

| Property | ASTM Standard | Description | Bio-Based Hydraulic Fluids (Vegetable Oil-Based) | Mineral-Based Hydraulic Fluids (Petroleum-Derived) | Bio-hydraulic fluids from palm oil using (Graphite, eggshell and snail shell values respectively) |
|---|---|---|---|---|---|
| Dynamic Viscosity | ASTM D7042 | Measures dynamic viscosity (cP) at 40°C/100°C. Convertible from kinematic viscosity (ASTM D445) via density (cP = cSt × ρ). | 20–50 cP at 40°C (kinematic: 20–50 cSt, ρ ~0.9 g/cm³). ISO VG 32–68 equivalents. | 25–70 cP at 40°C (kinematic: 28.8–74.8 cSt, ρ ~0.87 g/cm³). ISO VG 32, 46, 68. | 31.95 34.78 cP at (40°C) |
| Pour Point | ASTM D97 | Lowest temperature at which fluid flows, critical for cold-weather performance. | -50 to -30°C (additives improve low-temperature flow). | -30 to -15°C (higher due to paraffin content). | -44.8, -41.7, -40.5°C |
| Flash Point | ASTM D93 | Temperature at which vapours ignite, indicating fire safety. | 200–300°C (higher due to ester structures). | 150–220°C (lower due to volatile hydrocarbons). | 246–257°C |
| Biochemical Oxygen Demand (BOD) | No ASTM Standard (Suggest ISO 10708) | Oxygen consumed by microorganisms degrading organic matter, indicating biodegradability. | 5–20 ppm (high biodegradability, context-dependent). | 0.5–5 ppm (low biodegradability). | 8.04–8.23 ppm |

## 5.0 Conclusions

This study successfully demonstrates the formulation of bio-hydraulic fluids from palm oil, utilising eggshell and snail shell as sustainable friction modifiers alongside graphite, with viscosity optimised through Response Surface Modelling (RSM). The XRD results revealed eggshells and snail shells possessed mineralogical properties (calcite and aragonite respectively), confirming their suitability as friction modifiers and anti-wear agents of hydraulic fluids,

indicating they can compete favourably with graphite in the friction modification function of the bio-hydraulic fluid. Offers a cost-effective and eco-friendly alternative to conventional graphite. Glycerol derived from palm oil exhibited functional groups with polar atoms, single bonds, and double bonds, suggesting suitability for bio-hydraulic fluid formulation. The FTIR spectra of the separately produced bio-hydraulic fluids identified functional groups (alkanes, heteroatoms) essential for lubricity. A quadratic model described the relationship between viscosity and considered factors (glycerol/methanol ratio, dosage, temperature, and time). The optimised bio-hydraulic fluid viscosity and its process conditions were given as: dynamic viscosity 34.78, 31.95, 33.48 cP; glycerol/methanol ratio 20:20:20; eggshell dosage 0.6/0.6/0.6 g; temperature 60/60/60°C; and time 30/30/30 min, for graphite, eggshell, and snail shell respectively. Three-dimensional plots of the viscosity of the bio-hydraulic fluids revealed parabolic curves, which are typical for quadratic models. The formulated bio-hydraulic fluids demonstrate superior performance in pour point, flash point, and BOD compared to mineral-based fluids while matching bio-based fluid standards for viscosity. These properties, validated by ASTM standards, confirm the potential of palm oil, eggshell, and snail shell as sustainable raw materials for hydraulic fluid applications. The high biodegradability and reduced environmental impact align with ISO 15380 (HEES) standards for environmentally acceptable fluids. The RSM model's predictive accuracy ($R^2 \approx 0.99$) underscores its potential for precise process optimisation in bio-lubricant production. This work advances sustainable lubricant technology, paving the way for broader waste valorisation in industrial applications

## 6.0 Recommendations

Building on these findings, subsequent work will: Investigate enzymatic solvent systems for enhanced process sustainability and Expand feedstock options to include underutilized agricultural wastes (e.g., cassava peels, rice husks). XRD analysis to ensure accurate mineralogical characterisation.

## Acknowledgements

The authors acknowledges my father Benneth Tochukwu Ifediorah and my sibling Ambassador Isreal Chinonso Ifediorah, for their encouragement and motivation throughout this research work. We acknowledges the Chemical engineering Laboratory, Chemical Engineering Department, Chukwuemeka Odumegwu Ojukwu University, Anambra State, Nigeria.

## Nomenclature

FT-IR = Fourier transform infrared spectroscopy
XRD = X-ray Diffractometer
FM = Friction modifiers
R2 = Coefficient of Determination (Measures how well the model fits the data).
BOD (ppm) = Biochemical oxygen demand
$DO_i$ = Initial dissolve oxygen
$DO_f$ = Final dissolve oxygen after five days
P = Fraction of the sample
v = Volume of sample ($cm^3$)

## References

Alang, M. B., Ndikontar, M. K., Sani, Y. M., Ndifon, P. T., 2018. Synthesis and characterisation of a biolubricant from cameroon palm kernel seed oil using a locally produced base catalyst from plantain peelings. Green and Sustainable Chemistry, 8(3), 275-287.

Akinpelu, K.B., Onukwuli O.D., Eluno, E. E., 2021. Optimizing process parameters of palm oil bleaching on locally prepared animal bone based activated carbon using response surface methodology. Environmental Quality Management, 30(5).

Azinta, C. O., Mbah G. O., Omotioma M. 2021. Analysis of Effects of Foreign Clay and Local Clay Additives on Viscosity of Water Based Drilling Mud. Journal of Engineering Research and Reports, 21(4), 60-67.

Behzad, Kamyab., Ramon, Beims., Darren, W. Chambers., Amarjeet S., Bassi, Chunbao Xu., 2024. Sustainable production of high-performance bio-based hydraulic fluids from vegetable oils: Recent advances, current challenges, and future perspectives, Biomass and Bioenergy, Volume 183, 107160,ISSN 0961-9534,

Deuster, S. & Schmitz, K. (2021). Bio-Based Hydraulic Fluids and the Influence of Hydraulic Oil Viscosity on the Efficiency of Mobile Machinery. Sustainability, 13, 7570, 1-22.

Dumancas, G., Patel, V. Viswanath, L., Maples, R., Subong, B. J. 2016. Castor Oil: Properties, Uses, and Optimization of Processing Parameters in Commercial Production. Lipid Insights, 6, 1-12.

Esonye, C., Onukwuli, O. D., Ofoefule A. U. 2019. Optimization of methyl ester production from Prunus Amygdalus seed oil using response surface methodology and artificial neural networks. Renewable Energy, 130, 61-72.

Eze, C. C. (2016). Formulation and Production of Bio-Hydraulic Fluid as an Alternative to Mineral fluids for Automobiles. American Journal of Engineering Research (AJER), 5 (10), 147-151.

Jedli, H., Almonnef, M., Rabhi, R.; Mbarek, M.; Abdessalem, J., Slimi, K., 2024. Activated Carbon as an Adsorbent for CO2 Capture: Adsorption, Kinetics, and RSM Modeling. ACS Omega, 9 (2), 2080– 2087.

Jonah, C, U., Stanley, O., Chidozie C. W., Okechukwu, D. O. 2021. Computational modeling and multi-objective optimization of engine performance of biodiesel made with castor oil. Cleaner chemical engineering 5, 45-47.

Khan, N., Mushtaq, A., Khan, R. M., Ali, Z. U. 2023. Production of Bio-lubricant from Neem Oil. Pakistan Journal of Scientific & Industrial Research Series A. Physical Sciences, 66(3), 281-290.

Pindit, K.N., Ngamcharussrivichai, P., Kitchaiya, C., Eaimlamai, W., Kitchaiya., 2021. Biolubricant basestocks synthesis using 5-step reaction from jatropha oil, soybean oil, and palm fatty acid distillate Industrial Crops and Products. Jurnal Teknologi, 170, 112817.

Twin Specialties Corp. (n.d.). What are friction modifiers? Retrieved from https://www.twinoils.com/news/what-are-friction-modifiers/.

Marcel, K. N.; Rosemonde, Y.E.S.; Patricia, K.A.; Alexandre, Z.B.F.G.; Ambroise, A.N.; Ernest, A.K. 2020. Evaluation of the Nutritional Potential of Snail (Achatina spp) Meat in Rat. Eur. Sci. J. 16, 111–121.

Malik, M.A.I., M.H, Rashid., M.T, Alam., M.R, Islam., M.S, Hossain., M.A. Hashim., 2023. A review of recent advances in the synthesis of environmentally friendly, sustainable, and nontoxic bio-lubricants: recommendations for the future implementations Environmental Technology & Innovation, 30, 103-169.

Jabal, M.H., Abdul-Zahra, A.A., Abdulraof, H.A., 2020. Performance features of the sunflower seeds oil as a hydraulic bio fluid under various normal loads. Jurnal Teknologi, 82(4), 137–144.

Mignardi, S., Archilletti, L., Medeghini, L., 2020. Valorization of Eggshell Biowaste for Sustainable Environmental Remediation. Sci Rep 10, 2436.

Nnanwube, I. A., Onukwuli D. O. 2020. Modeling and optimization of galena dissolution in a binary solution of nitric acid and ferric chloride using artificial neural network coupled with genetic algorithm and response surface methodology. South African Journal of Chemical Engineering, 32, 68-77.

Attia, N.K., El-Mekkawim M.A., Elardy, E.A., Abdelkader, E.A., 2020. Chemical and rheological assessment of produced biolubricants from different vegetable oils Fuel. Cleaner, 271, 117-578.

Onukwuli O. D. and Omotioma M. (2016), Optimization of the Inhibition Efficiency of Mango Extract as Corrosion Inhibitor of Mild Steel in 1.0M $H_2SO_4$ using Response Surface Methodology. Journal of Chemical Technology and Metallurgy, 51 (3), 302 – 314.

Rahim, M. Z., 2023. Development of bio-lubricants using glycerol esters from palm oil: GCMS analysis and tribological performance. Tribology International, 4, 54-57.